molecules

MDPI

Review

MXene-Based Photocatalysts in Degradation of Organic and Pharmaceutical Pollutants

Siavash Iravani [1,*] and Rajender S. Varma [2,*]

[1] Faculty of Pharmacy and Pharmaceutical Sciences, Isfahan University of Medical Sciences, Isfahan 81746-73461, Iran
[2] Regional Centre of Advanced Technologies and Materials, Czech Advanced Technology and Research Institute, Palacký University in Olomouc, Šlechtitelů 27, 783 71 Olomouc, Czech Republic
* Correspondence: siavashira@gmail.com (S.I.); Varma.Rajender@epa.gov (R.S.V.)

Abstract: These days, explorations have focused on designing two-dimensional (2D) nanomaterials with useful (photo)catalytic and environmental applications. Among them, MXene-based composites have garnered great attention owing to their unique optical, mechanical, thermal, chemical, and electronic properties. Various MXene-based photocatalysts have been inventively constructed for a variety of photocatalytic applications ranging from pollutant degradation to hydrogen evolution. They can be applied as co-catalysts in combination with assorted common photocatalysts such as metal sulfide, metal oxides, metal–organic frameworks, graphene, and graphitic carbon nitride to enhance the function of photocatalytic removal of organic/pharmaceutical pollutants, nitrogen fixation, photocatalytic hydrogen evolution, and carbon dioxide conversion, among others. High electrical conductivity, robust photothermal effects, large surface area, hydrophilicity, and abundant surface functional groups of MXenes render them as attractive candidates for photocatalytic removal of pollutants as well as improvement of photocatalytic performance of semiconductor catalysts. Herein, the most recent developments in photocatalytic degradation of organic and pharmaceutical pollutants using MXene-based composites are deliberated, with a focus on important challenges and future perspectives; techniques for fabrication of these photocatalysts are also covered.

Keywords: photocatalysis; MXenes; pharmaceutical pollutants; photocatalytic degradation; pollutants; MXene-based nanocomposites

Citation: Iravani, S.; Varma, R.S. MXene-Based Photocatalysts in Degradation of Organic and Pharmaceutical Pollutants. *Molecules* **2022**, *27*, 6939. https://doi.org/10.3390/molecules27206939

Academic Editors: Madalina Ciobanu and Gabriela Petcu

Received: 27 September 2022
Accepted: 12 October 2022
Published: 16 October 2022

1. Introduction

Two-dimensional (2D) nanomaterials have been broadly explored by researchers for their unique catalytic and biomedical applications [1–5]. Among them, MXene-based composites have received immense attention owing to their attractive physicochemical features [6–8]. MXenes (with a typical formula of $M_{n+1}X_nT_x$, n = 1–3) have been widely synthesized using a variety of bottom–up and top–down strategies [9–12], including acid etching, chemical vapor deposition, electrochemical etching, molten salts etching, hydrothermal method, solvothermal techniques, ball-Milling, ultrasonic synthesis, pyrolysis approaches, among others [13–17]. However, several aspects pertaining to the application of non-/less-toxic agents, the optimal environmentally benign conditions, the improvement of stability/structural defects, the oxidation of MXenes, delamination methods, and the elimination of Al etching by-products ought to be further explored [18–23]. MXene-based structures with a large surface area, surface controllable chemical characteristics, regular planar structures, unique optical/thermal features, hydrophilicity, excellent metal conductivity, and abundant derivatives have been widely studied for photocatalytic degradation of pollutants (Figure 1) [24–28]. They have shown excellent potential for eliminating pollutants through interfacial chemical transformation and sorption, along with catalytic removal and photocatalytic degradation capabilities [29,30].

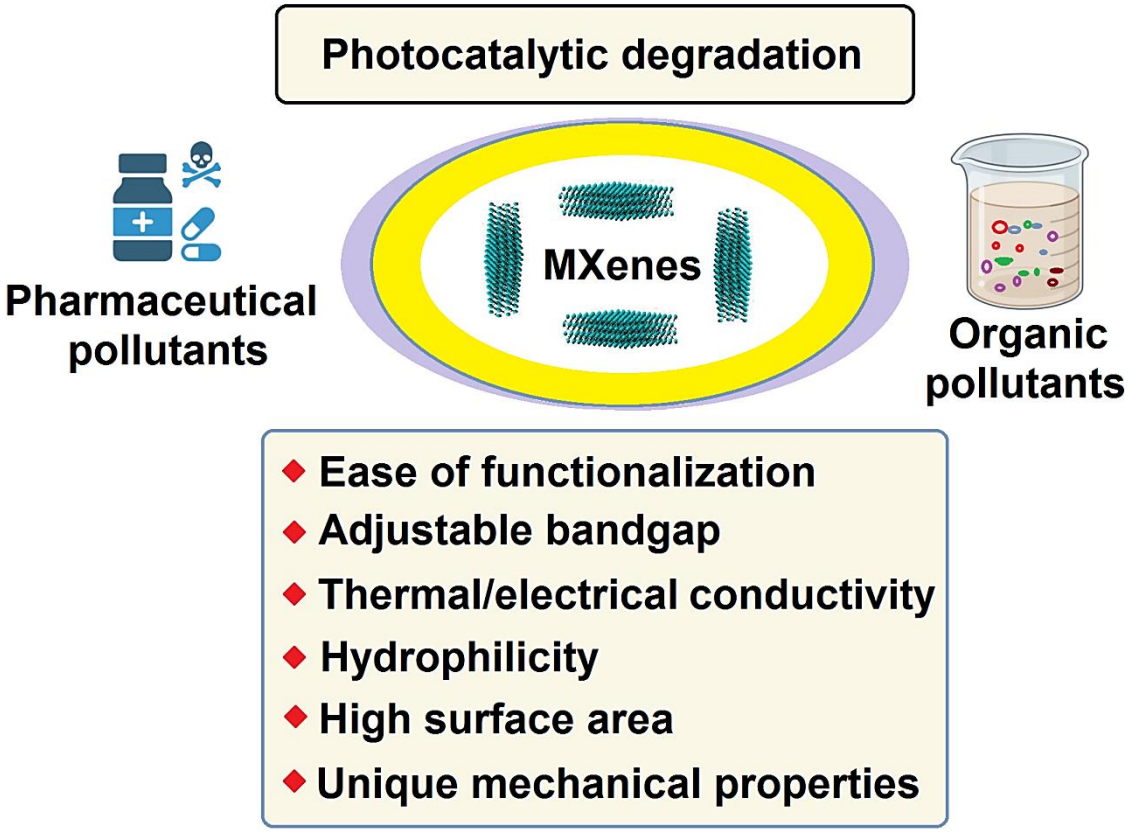

Figure 1. MXenes with unique properties for photocatalytic degradation of pharmaceuticals and organic pollutants.

MXenes with high conductivity and unique lamellar nanostructures can enhance the photo-electrocatalytic capabilities of composites as co-catalysts [31,32]. Among MXenes, titanium carbide ($Ti_3C_2T_x$) with promising photocatalytic performance, flexible structure, electronic features, and semimetal nature has been broadly studied for environmental applications, especially photocatalytic degradation of hazardous pollutants (Table 1) [33]. MXenes with surface functional groups such as F, OH, and O are capable of strong interaction with other semiconductors to generate efficient heterojunctions. MXenes (Ti_3C_2) successfully adsorb the hazardous pollutants and organic dyes, providing effective adsorbents for the removal of dyes from wastewaters [28,34]; their layered and porous structures facilitate their adsorption and storage capabilities [19,35]. Several hybrid structures have been constructed from MXenes for photocatalytic purposes [36,37]. For instance, rice crust-like hybrid structures were constructed from zinc oxide (ZnO) and MXene ($Ti_3C_2T_x$) with excellent photocatalytic performance, showing large surface area, Schottky barrier generation, and ideal band alignment. Besides, these hybrid photocatalysts showed excellent recyclability and stability [36]. Herein, the most recent developments pertaining to the photocatalytic degradation of organic and pharmaceutical pollutants are deliberated, with a focus on important challenges and future perspectives; important techniques for synthesis of these photocatalysts are also covered.

Table 1. Some selected MXene-based composites with photocatalytic degradation performance towards organic and pharmaceutical pollutants.

MXene-Based Photocatalysts	Pollutants	Advantages/Properties	Refs.
Carbon nitride coupled with Ti_3C_2-Mxene derived amorphous titanium (Ti)-peroxo heterojunction	Rhodamine B and tetracycline	- High reusability and stability - Superb photocatalytic degradation efficiency over Rhodamine B (~97.22%) and tetracycline (~86.34%) under visible light irradiation ($\lambda > 420$ nm), within 60 min	[38]
Carbon/Ti-based oxide nanocomposites/MXenes ($Ti_3C_2T_x$)	Methylene blue	- Significant removal of methylene blue (~90%) under visible light illumination, within 1 h. - Narrowed band-gap with suitable electronic conductivity - Large specific surface area - Excellent efficiency of charge separation with improved absorption capabilities	[39]
Rod-like Nb_2O_5/Nb_2CT_x composites	Rhodamine B and tetracycline	- High photocatalytic degradation of Rhodamine B (~98.5%, 120 min) and tetracycline (~91.2%, 180 min) under visible light irradiation - High photoactivity and cycle stability	[40]
$TiO_2/Ti_3C_2T_x$	Carbamazepine	- High photocatalytic degradation of carbamazepine (~98.67%) under UV light irradiation - •OH and $\bullet O_2$ attacked the carbamazepine molecule during the photocatalytic degradation	[41]
Lanthanum (La)- and manganese (Mn)-co-doped bismuth ferrite/MXene (Ti_3C_2) composites	Congo red	- Fast degradation of organic dye molecules - ~92–93% degradation of dye pollutant	[42]
MXene (Ti_3C_2)/Ag_2ZnGeO_4 Schottky heterojunctions	Acid red 1	- Enhanced visible light photocatalytic performance - Improved formation of superoxide radicals as the chief active species - Efficient charge separation	[43]
MXene-based catalysts (TiO_2/Ti_3C_2) modified with silver (Ag) particles	Nitrate	- The photoelectron density as well as the carrier separation of the catalysts could be improved by applying Ag particles - The rate of nitrate elimination ~96.1%; the selectivity towards nitrogen was ~92.6% - High photocatalytic removal efficiency (~89%) towards nitrate, even after 5 cycles	[44]

Table 1. *Cont.*

MXene-Based Photocatalysts	Pollutants	Advantages/Properties	Refs.
Magnetic-$Ti_3C_2T_X$	Diclofenac	- Enhanced degradation of diclofenac due to the formation of active radicals, including the hydroxyl radical and reactive chlorine species - Excellent stability and photodegradation efficiency during seven consecutive degradation reaction cycles	[45]
Ti_3C_2/*g*-C_3N_4	Phenol	- 98% phenol removal efficiency - 32.1% phenol could be degraded under dark conditions owing to the capability of MXenes in storing additional photo-generated electrons under light irradiation and releasing them when exposed to electron acceptors in dark conditions	[46]
$CuFe_2O_4/Ti_3C_2$	Sulfamethazine	- The synergistic degradation effects under visible light - The breaking of S–N bonds could be detected; the oxidation of aniline and deamination were dominated by attacking •OH	[47]
Bismuth/bismuth oxychloride (Bi/BiOCl) microspheres/Ti_3C_2	Ciprofloxacin	- Excellent reusability in the 5 cycles of ciprofloxacin degradation - High photocatalytic performance	[48]

2. Techniques for the Synthesis of MXene-Based Photocatalysts

Several techniques have been introduced for synthesizing a variety of MXene-based (nano)photocatalysts, including electrostatic self-assembly, calcination processes, hydrothermal treatment, mechanical/ultrasonic mixing, solvothermal treatment, etc. [49,50]. Among them, mechanical/ultrasonic mixing techniques have the advantage of simplicity when preparing MXenes; robust mechanical stirring and/or high-power ultrasonic vibration has been typically applied for retaining the intimate contact between MXenes and photocatalysts [49]. In one study, hydrogels of $Ti_3C_2T_x$ were prepared through the stirring of MXenes and graphene oxide colloidal solutions with Eosin Y solution for 0.5 h; after that the mixtures were kept at 70 °C with the protection of N_2 gas [51]. In another study, cadmium sulfide (CdS)/MXene (Ti_3C_2) composites were synthesized using an electrostatic self-assembly technique. Accordingly, MXene nanosheets and CdS nanowires were well-combined using electrostatic attraction, and the nanowires were successfully distributed on MXene nanosheets [52]. Notably, hydrothermal and solvothermal methods have been broadly applied for producing MXene-based composites. For instance, an in situ metal organic framework (MOF)-derived technique was deployed for synthesizing Co-Co layered double hydroxide/$Ti_3C_2T_X$ nanosheets with photocatalytic potentials using a solvothermal method [53]. Besides this, Ti_3C_2/Bi_2WO_6 composites were synthesized using electrostatic attraction and a hydrothermal method; these composites exhibited efficient photocatalytic performance with enhanced CO_2 adsorption potential [54].

In etching techniques, a variety of etchants can be applied for fabricating MXenes, including hydrogen fluoride (HF), lithium fluoride (LiF) plus HF, zinc chloride ($ZnCl_2$), etc. Different MXenes could be obtained by adjusting the concentration and duration of the etching process [55,56]. For instance, the replacement reaction method was deployed for synthesizing Zn-based MAX and Cl-terminated MXenes using $ZnCl_2$ Lewis acidic

molten salt. However, several challenging issues ought to be considered regarding higher temperature, poor crystallinity, purity requirements, and high energy consumption [57]. In addition, several chemical vapor deposition techniques have been reported for controlled manufacturing of MXene epitaxial films with multilayers [58]. In one study, 2D ultrathin α-Mo_2C crystals with a large surface area were synthesized through a chemical vapor deposition technique, exhibiting high quality with defect-free structures [59]. Besides this, 2D Mo_2C was directly synthesized on grown graphene (in situ) deploying a one-step copper-catalyzed chemical vapor deposition technique [60]. Despite the advantages of chemical vapor deposition techniques such as the fabrication of MXenes with low impurity and defects, low yield of production and complex treatment pathways are some of their crucial drawbacks; with additional modifications, these techniques can be further improved [61].

3. Photocatalytic Degradation of Organic and Pharmaceutical Pollutants

Photocatalysis is considered a relatively safer and low-cost strategy for the elimination of hazardous pollutants [37,62,63]. In this context, MXenes with distinctive lamellar structures and remarkable conductivity can be applied as nano-adsorbents to remediate environmentally toxic pollutants, and also as co-catalysts for improving photocatalytic degradation potential of the other composites in their photocatalytic performances [13,64]; several studies have focused on photocatalytic degradation of dyes, heavy metals, and pharmaceutical pollutants. For instance, MXene/TiO_2 nanocomposites were constructed for photocatalytic degradation of organic pollutants [65]. In one study, MXene (Ti_3C_2) nanosheets decorated with copper sulfide (CuS) particles were fabricated using a hydrothermal treatment technique to enhance the catalytic persulfate activation under light, showing excellent reactivity for rapid elimination of Orange II; the CuS@MXene composites exhibited high stability even after 4 cycles of reusability evaluation [66]. The dosage of persulfate and initial pH of solution were the chief parameters affecting the elimination rate of pollutant; $^1O_2$ was the primary reactive species for removing Orange II using the nanocomposite [66].

After the formation of magnetic heterojunctions of α-Fe_2O_3/$ZnFe_2O_4$ through a simple hydrothermal fabrication technique, the photocatalyst was prepared utilizing MXenes as co-catalysts through ultrasonic-assisted self-assembly to disperse obtained magnetic heterojunctions on the surface of MXene (Ti_3C_2) (Figure 2) [67]. These photocatalysts exhibited improved photocatalytic activity in elimination of rhodamine B and toxic Cr (VI) in water with reusability and high conductivity advantages [67]. In another study, MXene (Ti_3C_2)/MoS_2 nanocomposites with a specific surface area were prepared via a hydrothermal approach, showing efficient photocatalytic organic pollutant degradation [68]. These MXene-based nanophotocatalysts with excellent removal of methyl orange pollutants exhibited improved optical absorption potential. Notably, the incorporation of MXenes with MoS_2 nanosheets could improve the photocurrent response and reduce the electrochemical impedance, causing an improvement in electron transfer of excited semiconductors along with an inhibition in charge recombination [68].

The hybridization strategies can help to enhance the photocatalytic degradation efficiency of MXenes and their derivatives [16]. Several studies have focused on hybridization of MXenes with other materials, including graphene and its derivatives, metal–organic frameworks (MOFs), polymers (cellulose or chitosan), carbon nanotubes, carbon dots, etc. [69–71]. MXenes hybridized with graphene and their derivatives have been studied due to their fascinating properties. In one study, graphene oxide-based nanofiltration membranes intercalated with TiO_2 nanomaterials were prepared by the in situ oxidation of MXene nanosheets; ensued composites could remove the organic dyes with high efficiency (~97%) [72]. In addition, graphitic carbon nitride (g-C_3N_4) and TiO_2 were attached to the graphene layers, and then were applied for synthesizing photocatalysts using MXenes (Ti_3C_2) via a simple calcination process (in situ); these photocatalysts had excellent degradation potential for pharmaceutical and organic pollutants under visible light irradiation, including tetracycline, ciprofloxacin, rhodamine B, and bisphenol A [73]. Notably, these sta-

ble and reusable photocatalysts had improved visible light adsorption and photo-generated carrier separation. The visible light photocatalytic degradation rate was significantly improved, because of the synergist effects and robust interactions among g-C_3N_4, graphene, and TiO_2 for the separation and accumulation of g-C_3N_4 electrons with superb reduction potential and TiO_2 holes with remarkable oxidation ability, thus making them as promising candidates for pharmaceutical degradation/elimination [73]. Xu et al. [74] constructed MXene@Fe_3O_4@chitosan composites using an ultrasonic self-assembly technique for removing Congo red (Figure 3); chitosan with adsorption capacity of 620.22 $mg{\cdot}g^{-1}$ was deployed for improving the adsorption capacity. Accordingly, the adsorption surveyed Langmuir isotherm model, and the related kinetics were detected to mainly follow the quasi-secondary rate kinetics. Notably, it was revealed that adsorption was endothermic, entropy-driven, and based on the thermos-dynamically spontaneous process. The magnetic nanocomposites exhibited significant adsorption capacity under neutral or weakly acidic conditions; however, under alkaline conditions, they displayed very low adsorption capacity [74].

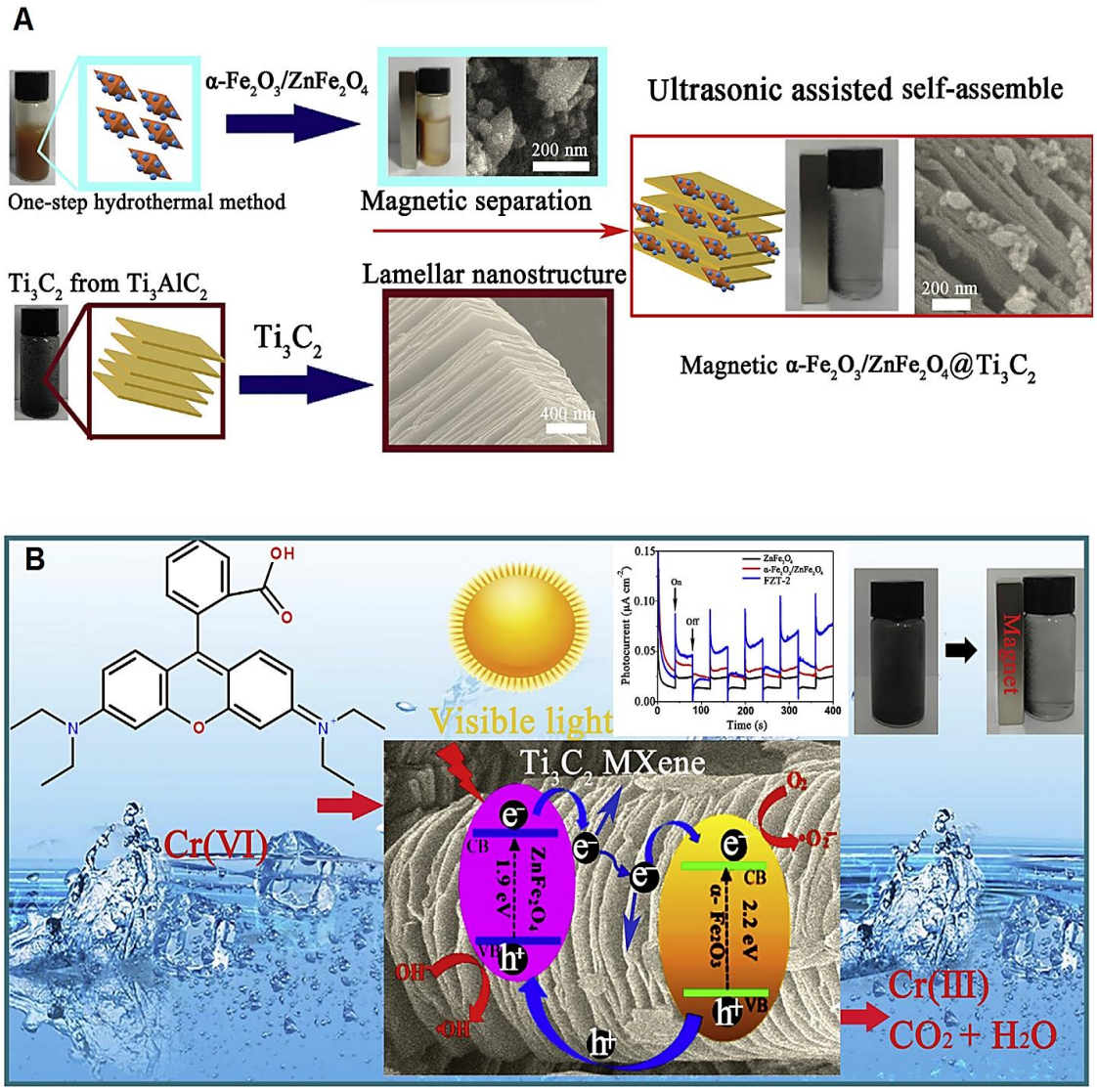

Figure 2. (**A**) The preparative process of magnetic α-Fe_2O_3/$ZnFe_2O_4$@MXene (Ti_3C_2) composites, with (**B**) mechanism of rhodamine B and toxic Cr (VI) photocatalytic removal in water. Adapted from Ref. [67] with permission. Copyright 2019 Elsevier.

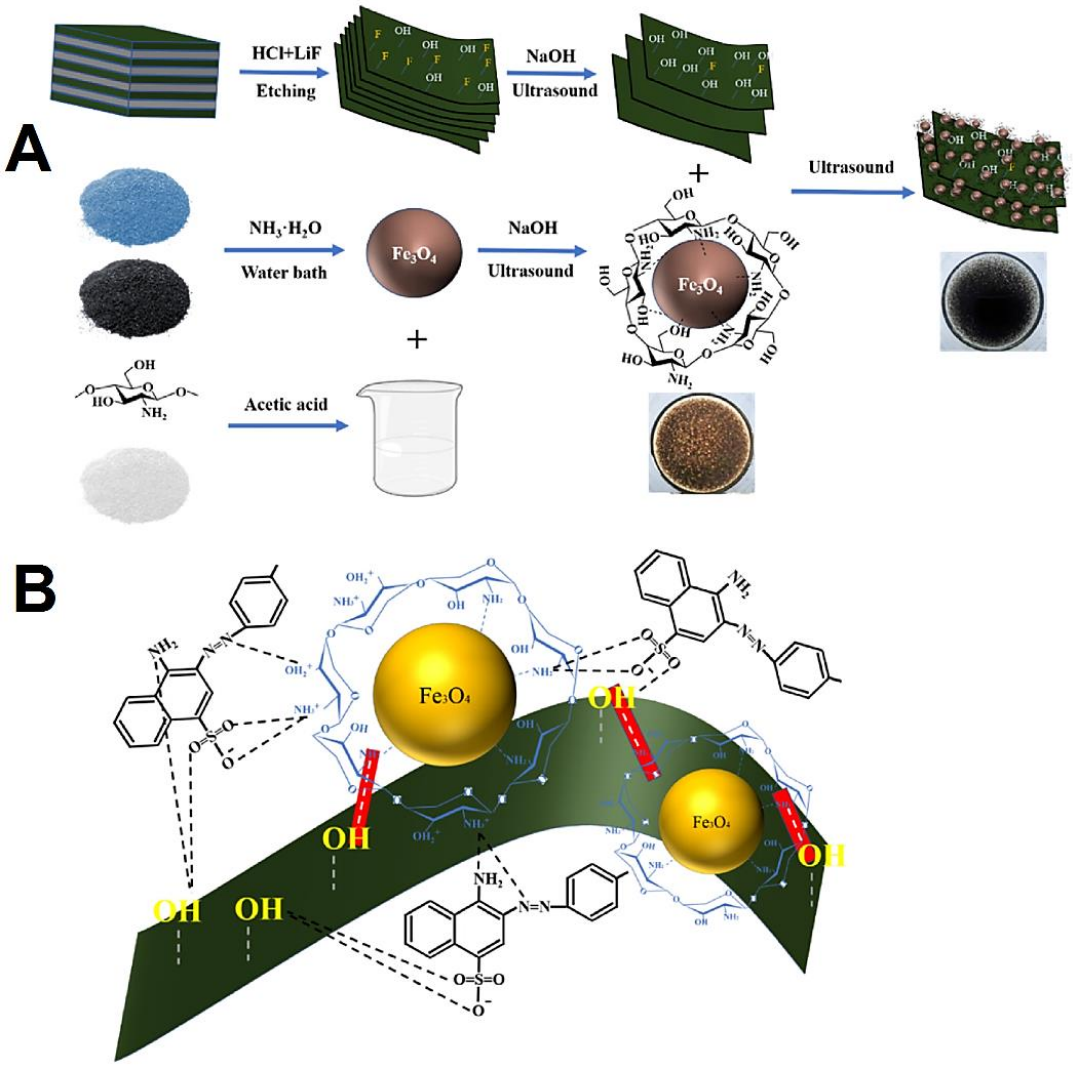

Figure 3. (**A**) The preparative process for MXene@Fe_3O_4@chitosan (CS) magnetic nanocomposites, with related adsorption mechanism (**B**). LiF: lithium fluoride. Adapted from Ref. [74] with permission. Copyright 2022 Elsevier.

Structures constructed from MXene (Ti_3C_2)/O-doped *g*-C_3N_4 Schottky-junction were reported through an in situ electrostatic assembly of negatively charged MXenes and positively charged O-doped *g*-C_3N_4 nanosheets. The obtained photocatalysts exhibited enhanced hydrogen evolution and photocatalytic activity due to the synergy between the compounds as well as the formation of a Schottky-junction [75]. In one study, ternary $Ti_3C_2T_x/Ti_3AlC_2$@Ag composite photocatalysts were fabricated for catalytic degradation of methylene blue, Rhodamine B, and methylene orange, with an efficiency of 99.7%, 98.9% and 99.3%, respectively (Figure 4) [76]. Synergistic effects could be obtained between Ag nanomaterials and partial etched Ti_3C_2Tx/Ti_3AlC_2 nanosheets, which were illustrated by transference of the photogenerated carriers and the formation of reactive oxygen species (ROS); these effects could additionally enhance the catalytic degradation performance [76].

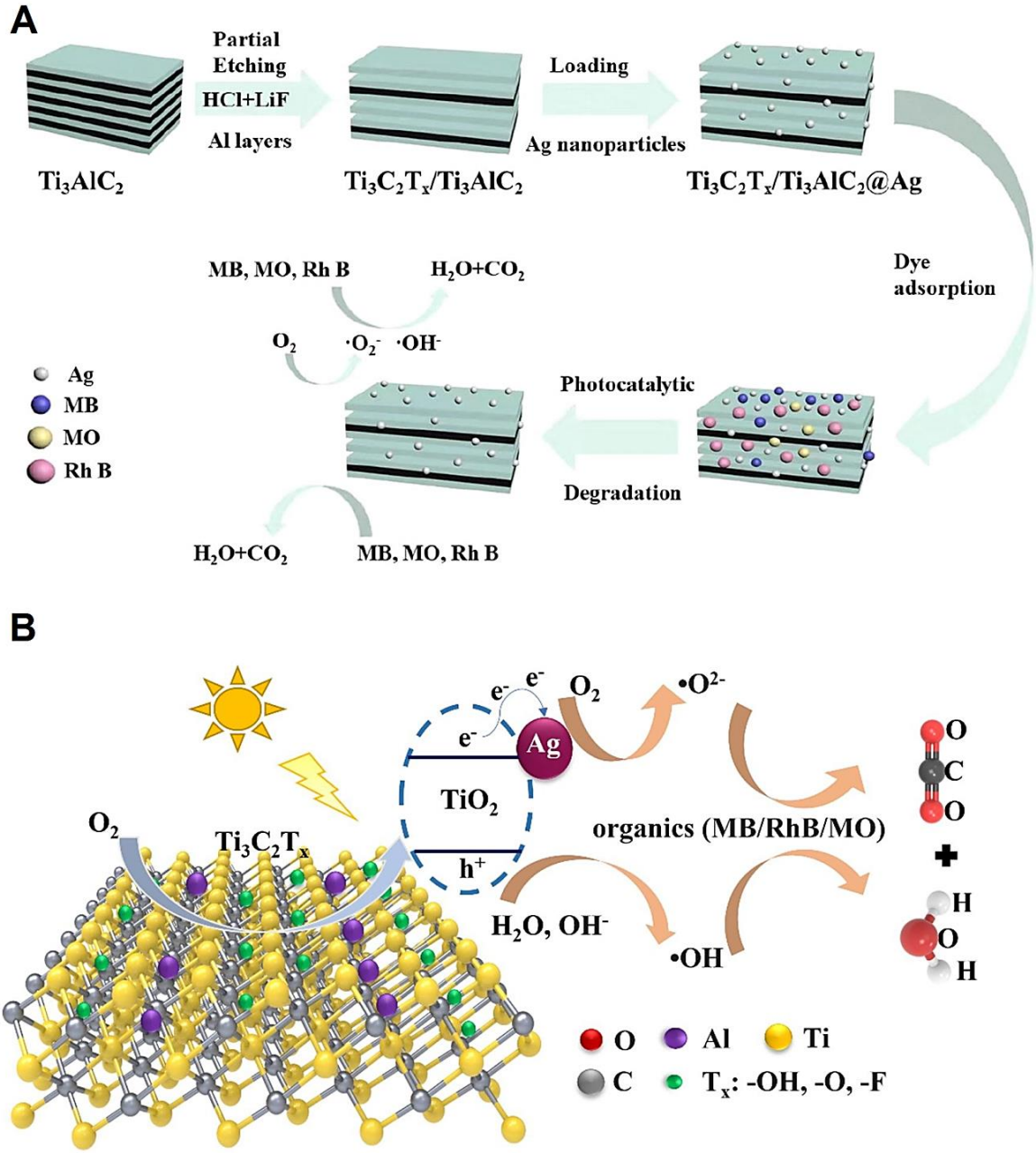

Figure 4. (**A**) The preparative process of ternary $Ti_3C_2T_x/Ti_3AlC_2$@Ag composites for the photocatalytic degradation of pollutants. (**B**) ROS and photodegradation reaction mechanisms. MB: methylene blue; RhB: Rhodamine B; MO: methylene orange. Adapted from Ref. [76] with permission. Copyright 2022 Elsevier.

MXene-based nanocomposites fabricated via catalytic chemical vapor deposition were hybridized with carbon nanotubes for photocatalytic removal of Rhodamine B, wherein the photocatalyst degradation efficiency for pure MXenes and MXene-carbon nanotube composites were found to be 60% and 75%, respectively. The hybrid composites exhibited good degradation efficiency for pollutants in successive cycles [77]. In addition, MXene-based composites comprising multi-layered MXene (Ti_3C_2) nanosheets and transition metal oxide nanomaterials, i.e., zinc oxide, bismuth molybdate and tin dioxide, were introduced for the catalytic removal of pollutants with high adsorption capacity towards methylene blue [78]. Accordingly, 150 mg L^{-1} of high concentration methylene blue solution and 20 mg L^{-1} of 4-chlorophenol solution were totally eliminated by adsorption and photocatalysis using these MXene-based photocatalysts for 4 h under visible light

irradiation. Studies on mechanisms revealed that hydroxyl and superoxide free radicals were reactive species in the degradation procedure; coupling transition metal oxide and MXene inhibited the recombination of photogenerated electron–hole pairs [78]. These MXene-based nanocomposites with synergistic removal of pollutants and strong adsorption thus offer themselves as promising photocatalysts for environmental pollution control.

The design of heterostructures can improve the catalytic performance of MXene-based photocatalysts, because of the triggered interfacial electron transfer [64]. In one study, the chimeric ZnO nanosheets with suitable carrier mobility were created on the accordion-shaped surface of MXenes (Nb_2C and V_2C) to obtain hierarchical ZnO/MXene heterostructures as photocatalysts for degradation of dyes [79]. These structures with good stability exhibited improved photocatalytic activity for degrading methylene blue; the degradation rate for ZnO/Nb_2C was ~62.62% and for ZnO/V_2C was found to be ~99.53, after UV irradiation within 120 min. The degradation rate endured at 58.6% and 97.3%, respectively, after 4 cycles, while it was only 22.0% for pure ZnO. This is because of the formed ZnO/MXene hierarchical structures with uniform active sites on their surfaces and porous structures, which prevented the aggregation of ZnO or MXenes. Notably, the heterostructures between ZnO and MXenes could abridge the carrier transfer pathway, facilitating the transfer of photo-generated electrons from the conduction band of ZnO to the conduction band of MXenes, and enhancing the efficiency of photocatalytic degradation [79]. This strategy can improve the catalytic activity of other 2D photocatalytic structures, paving a way for designing efficient photocatalysts. Sun et al. [80] developed MXene (Ti_3C_2)-bridged Ag/Ag_3PO_4 hybrid composites with Ti_3C_2 content-dependent photocatalytic performance for the degradation of MO and Cr(VI) reduction under visible light irradiation; the highest MO degradation efficiency could be obtained with 3 wt% Ti_3C_2 content after irradiation for 1 h. The mechanistic studies revealed that improved photocatalytic performance was associated with the synergetic effects that originated from Ag, Ag_3PO_4, and MXenes, enhancing visible light absorption and promoting separation and transfer of photo-generated electron–hole pairs [80].

Photocatalytic removal of pollutants of pharmaceutical origin and industrial wastes has been explored using MXene-based composites. For instance, MXene-Ti_3C_2/MoS_2 composites fabricated through a hydrothermal treatment technique were deployed for the photocatalytic removal of ranitidine and reduction of nitrosamine dimethylamine generation potential under visible light irradiation [81]. A heterojunction could be detected between MoS_2 and MXene, facilitating the separation of electron–hole pairs and charge transfer to improve photocatalytic activity. These composites demonstrated superior photocatalytic activity within ~60 min; the highest ranitidine degradation (~88.4%) and mineralization (~73.58%) efficiency, and the lowest nitrosamine dimethylamine formation potential of only ~2.01%. Mechanism studies revealed that active species such as $\bullet O_2^-$ radicals, h^+ and •OH radicals were responsible for degrading ranitidine, and •OH radicals were the chief active species that were responsible for photocatalytic performance [81]. Kumar et al. [82] developed MXene (Ti_3C_2) coupled *g*-C_3N_4 nanosheets based on plasmonic photocatalysts with good reusability (up to 3 cycles) for removal of pharmaceutical pollutants (cefixime) under visible light irradiation (Figure 5). After the optimization process, the photocatalysts containing 3 wt% MXenes could efficiently remove (~64.69%) cefixime under visible light exposure within 105 min. Mechanistic studies revealed that the presence of gold (Au) nanomaterials and MXenes in these nanocomposites could facilitate the outstanding charge carrier separation and increase the number of active sites, because of the generation of interfacial contact with *g*-C_3N_4 nanosheets. In addition, the plasmonic influence of Au nanomaterials improved the absorption of light photons, which could enhance the photocatalytic activity of these nanocomposites. Nanosheets of *g*-C_3N_4 were employed as semiconducting photocatalysts to efficiently harvest energy from visible light. Besides this, MXene nanosheets functioned as superb electron sinks and provided improved surface areas for the adsorption of hazardous pollutants; the application of MXenes as co-catalysts

in these nanocomposites facilitated the interfacial separation of charge carriers due to their excellent metallic conductivity and their abundant functional groups [82].

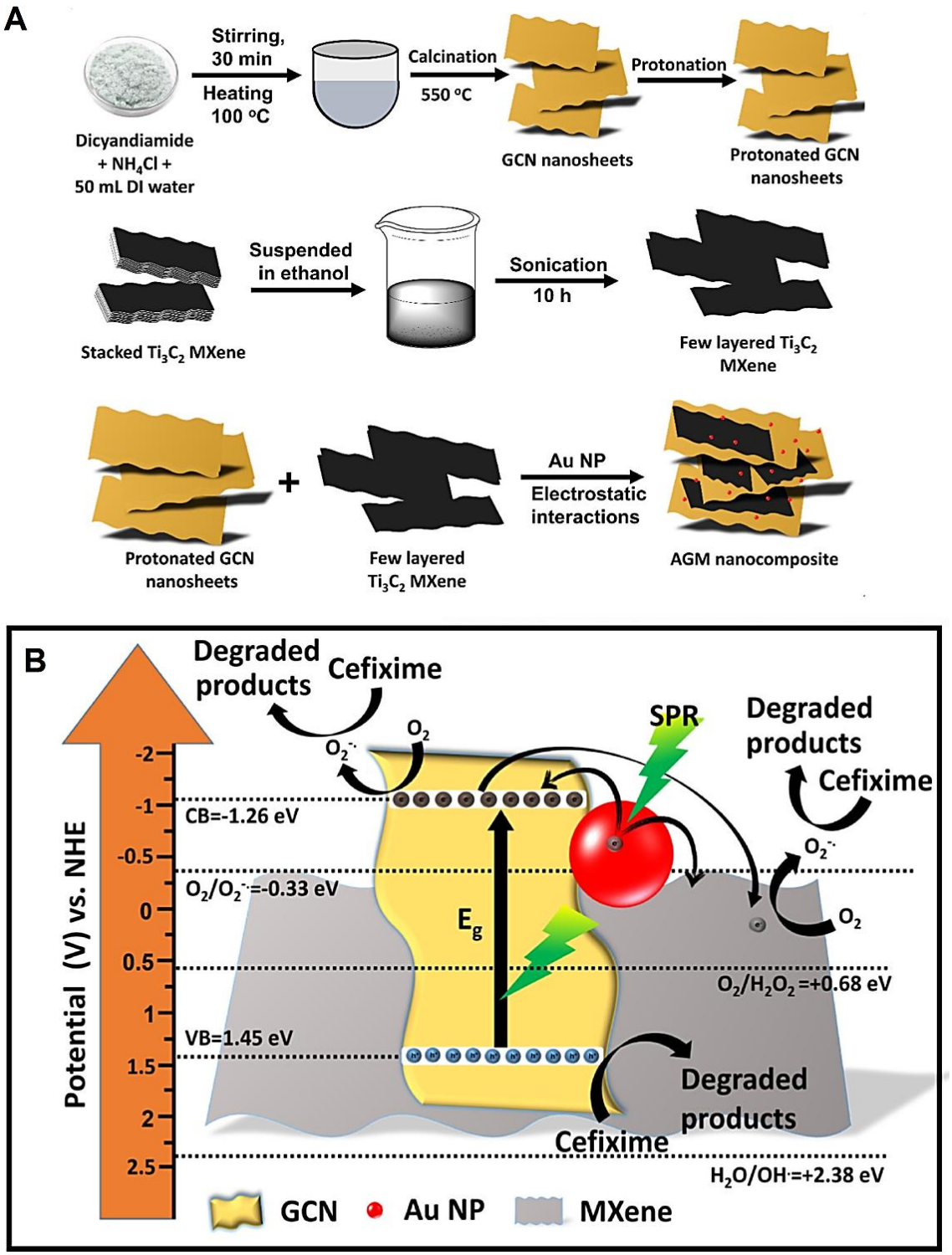

Figure 5. (**A**) The preparative process of Au nanomaterial-decorated *g*-C_3N_4/MXene (AGM) nanocomposites. (**B**) The photocatalytic decomposition mechanism for pharmaceutical pollutant (cefixime) using the designed nanocomposites under visible light illumination. GCN: *g*-C_3N_4; SPR: surface plasmon resonance. Adapted from Ref. [82] with permission. Copyright 2022 Elsevier.

The Z-scheme heterojunction-based photocatalyst has advantages of excellent electron–hole pairs separation efficiency, robust redox potential, and a broad light response range; the significant power of oxidization and reduction makes the Z-scheme heterojunction suitable for degradation of pollutants in water [83–85]. In one study, a Z-scheme heterojunction of *g*-C_3N_4/MXene (Ti_3C_2)/$MoSe_2$ was developed to achieve effective visible light-induced removal of enoxacin within 60 min [86]. Accordingly, MXene-stimulated interface electron separation could play an important role on degradation with high efficiency. Furthermore, MXene as a suitable mediator between *g*-C_3N_4 and $MoSe_2$ could effectively transfer the electron and inhibit its recombination. Notably, a Schottky-junction could be generated between MXene (the conductor) and *g*-C_3N_4/$MoSe_2$ (the semiconductor) to improve electron trapping; the trapped electron could stimulate the active species generation to enhance performance. During degradation, most commonly produced reactive species were $\bullet O_2^-$ and photogenerated electrons. The prepared photocatalyst exhibited promising degradation potential for other pollutants, including norfloxacin (~80%), moxifloxacin (~100%), ofloxacin (~100%), gatifloxacin (~65%), levofloxacin (~100%), and ciprofloxacin (~80%) [86]. Cao et al. [87] synthesized *g*-C_3N_4/TiO_2@Ti_3C_2 photocatalysts for effective visible light degradation of pollutants such as MO, revealing higher degradation rates with improved photocatalytic performance owing to the Z-type heterojunctions in the nanocomposites. It is because of the close interaction among the multilayer MXenes, perforated *g*-C_3N_4 flake with a large specific surface area, and oxidation-generated TiO_2 promoting the separation of photocatalytic carriers and catalytic reactions [87]. MXenes can highly improve the catalytic performance and stability of materials such as Ag_3PO_4 due to the abundant surface hydrophilic functional groups forming robust interfacial contact with Ag_3PO_4, facilitating the separation of carriers [88]. Additional radical •OH formation is also stimulated by the strong redox reactivity of surface Ti sites promoting multiple electron reduction reactions. In one study, a Schottky-junction generated at Ag_3PO_4-MXene (Ti_3C_2) interface suitably transferred electrons to the surface of the MXene by a built-in electrical field (Figure 6). The prepared composites displayed high photocatalytic degradation capabilities towards organic pollutants such as 2,4-dinitrophenol. The photocatalytic degradation of tetracycline hydrochloride was also maintained at ~68.4%, even after 8 successive cycles of reuse [88].

MXenes and MOFs have been hybridized for the photocatalytic degradation of pollutants. Long et al. [89] designed MXene (Ti_3C_2)/NH_2-MIL-88B(Fe) composites with a photocatalytic removal potential (>90%) towards methylene blue (50 ppm) within 30 min, along with the elimination of ~83.41% Rhodamine B (25 ppm) and 44.26% MO (20 ppm) within 120 min. The use of MXenes could help to prevent the agglomeration of MOFs and enhance the effective area of the composite material, acting as a photo-generated electron trap in the photocatalytic procedure for improving the charge separation efficiency of MOFs. The main mechanisms for dye removal entailed adsorption performance and the Schottky knot synergistic Fenton effect [89]. Since MXenes (Ti_3C_2) typically cannot be directly applied for a photocatalysis process and this matter may restrict their additional photocatalytic applications (especially in water), the proposed hybridization strategy using MOFs can help to improve their properties and functionalities. Another hybrid MXene-based photocatalyst was introduced using $NiCo_2S_4$ and MXene [90]. The photocatalyst with great photostability in 5 repetitive runs exhibited efficient degradation of rhodamine B (~100%) under visible light irradiation within 20 min. It was revealed that rhodamine B was primarily oxidized into non-toxic products such as H_2O, CO_2, and a few inorganic species, offering new opportunities for wastewater management with advantages of environmentally benign properties, cost-effectiveness, and the formation of non-toxic by-products [90].

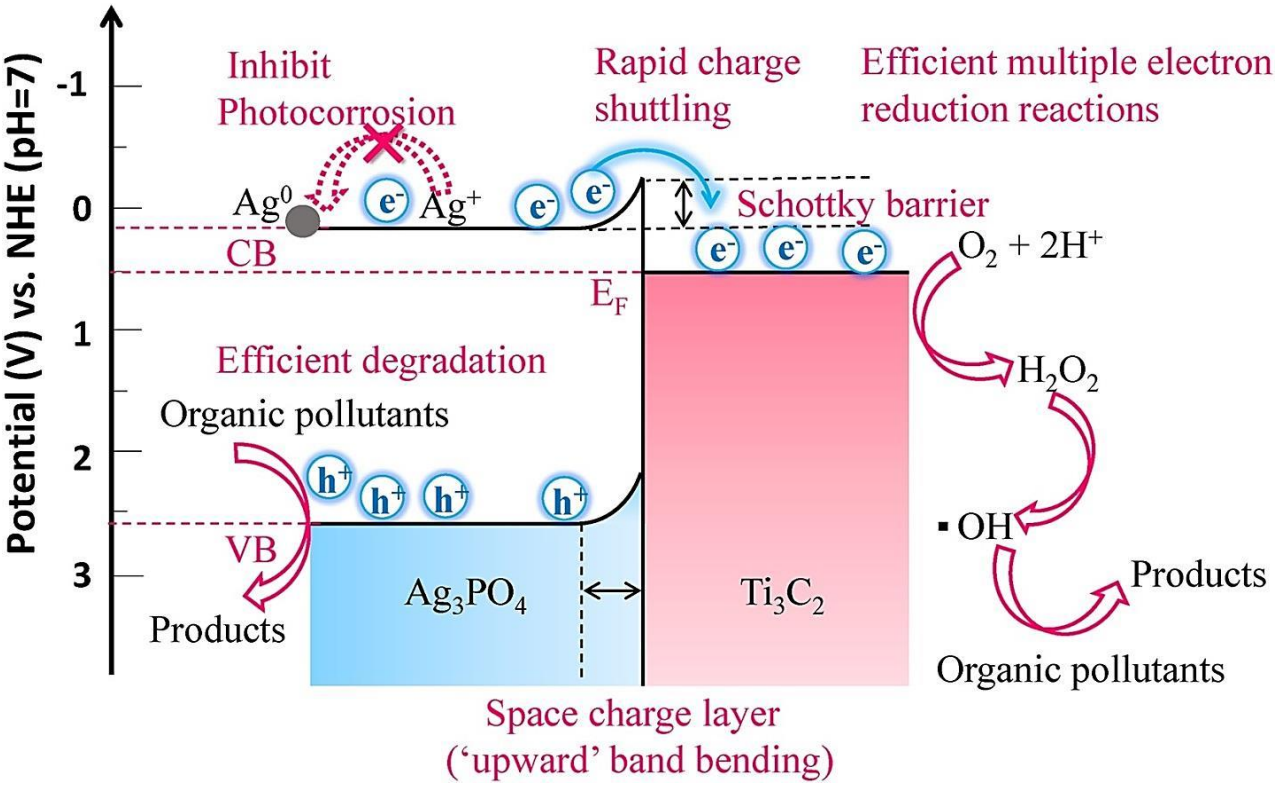

Figure 6. The possible mechanism of photocatalytic degradation of organic pollutants along with photo-corrosion inhibition of Ag_3PO_4/MXene (Ti_3C_2) Schottky catalysts. Adapted from Ref. [88] with permission. Copyright 2018 Elsevier.

4. Conclusions and Perspectives

MXene-based composites have attracted much attention as photocatalysts to degrade pollutants owing to their unique optical/thermal features, hydrophilicity, large surface area, surface controllable chemical properties, high chemical stability, regular planar architectures, high metal conductivity, and abundant derivatives. However, rapid recombination of photo-generated carriers typically may lead to a reduction in their photocatalytic functions. Designing a heterostructure can effectively improve the photocatalytic activities of MXene-based composites, because of the stimulated interfacial electron transfer. Notably, hybridization of MXenes with other materials such as MOFs, graphene, and polymers can help to improve their photocatalytic properties. In addition, MXenes with unique lamellar structures and excellent conductivity have been deployed as co-catalysts for enhancing the photocatalytic degradation capabilities of composites. Several aspects need to be systematically studied, including finding the functional groups' orientation on their surfaces. With advancements in photocatalysis and nanotechnology, MXenes and their derivatives with unique structural and physicochemical properties along with their biocompatibility, robust electrochemistry, and hydrophilicity can be employed as multifunctional candidates in novel environmental clean-up technologies for detection, mitigation, and elimination of various hazardous contaminants and organic/inorganic pollutants from environmental matrices; finding suitable techniques for improving the properties and functionality of MXene-based (nano)photocatalysts is one of the most important challenges ahead. More analytical and feasibility studies are still needed to move from laboratory-stage experiments to large/industrial-scale remediation of pollutants using MXenes. In addition, since $Ti_3C_2T_x$ is the most studied MXene for photocatalytic applications, it is suggested that future studies move towards the design of novel photocatalysts using other types of MXenes. The stability of MXenes still needs additional adjustments using suitable functionalization and/or post-production optimization processes. Large-scale production of MXene-based photocatalysts

is another crucial challenging issue; finding optimal reaction/synthesis conditions (pH, temperature, pressure, etc.) with advantages of simplicity, cost-effectiveness, eco-friendly properties, and repeatability can help move towards large-scale and commercial production of these photocatalysts.

Author Contributions: S.I. and R.S.V.: conceptualization; and writing—review and editing. All authors have read and agreed to the published version of the manuscript.

Funding: This research received no external funding.

Institutional Review Board Statement: Not applicable.

Informed Consent Statement: Not applicable.

Data Availability Statement: Not applicable.

Conflicts of Interest: The authors declare no conflict of interest.

References

1. Ihsanullah, I. MXenes (two-dimensional metal carbides) as emerging nanomaterials for water purification: Progress, challenges and prospects. *Chem. Eng. J.* **2020**, *388*, 124340. [CrossRef]
2. Tang, W.; Dong, Z.; Zhang, R.; Yi, X.; Yang, K.; Jin, M.; Yuan, C.; Xiao, Z.; Liu, Z.; Cheng, L. Multifunctional Two-Dimensional Core–Shell MXene@Gold Nanocomposites for Enhanced Photo–Radio Combined Therapy in the Second Biological Window. *ACS Nano* **2019**, *13*, 284–294. [CrossRef] [PubMed]
3. Murugan, C.; Sharma, V.; Murugan, R.K.; Malaimegu, G.; Sundaramurthy, A. Two-dimensional cancer theranostic nanomaterials: Synthesis, surface functionalization and applications in photothermal therapy. *J. Control. Release* **2019**, *299*, 1–20. [CrossRef] [PubMed]
4. Shafiee, A.; Iravani, S.; Varma, R.S. Graphene and graphene oxide with anticancer applications: Challenges and future perspectives. *MedComm* **2022**, *3*, e118. [CrossRef] [PubMed]
5. Shafiei, N.; Nasrollahzadeh, M.; Iravani, S. Green Synthesis of Silica and Silicon Nanoparticles and Their Biomedical and Catalytic Applications. *Comments Inorg. Chem.* **2021**, *41*, 317–372. [CrossRef]
6. Ji, Y.; Luo, Y. New mechanism for photocatalytic reduction of CO2 on the anatase TiO2(101) surface: The essential role of oxygen vacancy. *J. Am. Chem. Soc* **2016**, *138*, 15896–15902. [CrossRef] [PubMed]
7. Yang, C.; Tan, Q.; Li, Q.; Zhou, J.; Fan, J.; Li, B.; Sun, J.; Lv, K. 2D/2D Ti3C2 MXene/g-C3N4 nanosheets heterojunction for high efficient CO2 reduction photocatalyst: Dual effects of urea. *Appl. Catal. B* **2020**, *268*, 118738. [CrossRef]
8. Rhouati, A.; Berkani, M.; Vasseghian, Y.; Golzadeh, N. MXene-based electrochemical sensors for detection of environmental pollutants: A comprehensive review. *Chemosphere* **2022**, *291*, 132921. [CrossRef]
9. Feng, X.; Yu, Z.; Sun, Y.; Long, R.; Shan, M.; Li, X.; Liu, Y.; Liu, J. Review MXenes as a new type of nanomaterial for environmental applications in the photocatalytic degradation of water pollutants. *Ceram. Int.* **2021**, *47*, 7321–7343. [CrossRef]
10. Iravani, P.; Iravani, S.; Varma, R.S. MXene-Chitosan Composites and Their Biomedical Potentials. *Micromachines* **2022**, *13*, 1383. [CrossRef]
11. Iravani, S.; Varma, R.S. MXenes and MXene-based materials for tissue engineering and regenerative medicine: Recent advances. *Mater. Adv.* **2021**, *2*, 2906–2917. [CrossRef]
12. Iravani, S.; Varma, R.S. MXenes for Cancer Therapy and Diagnosis: Recent Advances and Current Challenges. *ACS Biomater. Sci. Eng.* **2021**, *7*, 1900–1913. [CrossRef] [PubMed]
13. Sreedhar, A.; Noh, J.-S. Recent advances in partially and completely derived 2D Ti3C2 MXene based TiO2 nanocomposites towards photocatalytic applications: A review. *Sol. Energy* **2021**, *222*, 48–73. [CrossRef]
14. Abbasi, Z.; Feizi, S.; Taghipour, E.; Ghadam, P. Green synthesis of silver nanoparticles using aqueous extract of dried Juglans regia green husk and examination of its biological properties. *Green Process. Synth.* **2017**, *6*, 477–485. [CrossRef]
15. Iravani, S. MXenes and MXene-based (nano)structures: A perspective on greener synthesis and biomedical prospects. *Ceram. Int.* **2022**, *48*, 24144–24156. [CrossRef]
16. Iravani, S.; Varma, R.S. MXenes in photomedicine: Advances and prospects. *Chem. Commun.* **2022**, *58*, 7336–7350. [CrossRef] [PubMed]
17. Rahman, U.U.; Humayun, M.; Ghani, U.; Usman, M.; Ullah, H.; Khan, A.; El-Metwaly, N.M.; Khan, A. MXenes as Emerging Materials: Synthesis, Properties, and Applications. *Molecules* **2022**, *27*, 4909. [CrossRef] [PubMed]
18. Shuck, C.E.; Ventura-Martinez, K.; Goad, A.; Uzun, S.; Shekhirev, M.; Gogotsi, Y. Safe Synthesis of MAX and MXene: Guidelines to Reduce Risk During Synthesis. *ACS Chem. Health Saf.* **2021**, *28*, 326–338. [CrossRef]
19. Sun, Y.; Meng, X.; Dall'Agnese, Y.; Dall'Agnese, C.; Duan, S.; Gao, Y.; Chen, G.; Wang, X.-F. 2D MXenes as co-catalysts in photocatalysis: Synthetic methods. *Nano Micro. Lett.* **2019**, *11*, 1–22. [CrossRef] [PubMed]
20. Wei, Y.; Zhang, P.; Soomro, R.A.; Zhu, Q.; Xu, B. Advances in the Synthesis of 2D MXenes. *Adv. Mater.* **2021**, *33*, 2103148. [CrossRef]

21. Wu, Q.; Li, N.; Wang, Y.; Xu, Y.; Wu, J.; Jia, G.; Ji, F.; Fang, X.; Chen, F.; Cui, X. Ultrasensitive and Selective Determination of Carcinoembryonic Antigen Using Multifunctional Ultrathin Amino-Functionalized Ti3C2-MXene Nanosheets. *Anal. Chem.* **2020**, *92*, 3354–3360. [CrossRef] [PubMed]
22. Wyatt, B.C.; Rosenkranz, A.; Anasori, B. 2D MXenes: Tunable Mechanical and Tribological Properties. *Adv. Mater.* **2021**, *33*, 2007973. [CrossRef] [PubMed]
23. Iravani, S.; Varma, R.S. MXenes in Cancer Nanotheranostics. *Nanomaterials* **2022**, *12*, 3360. [CrossRef] [PubMed]
24. You, Z.; Liao, Y.; Li, X.; Fan, J.; Xiang, Q. State-of-the-art recent progress in MXene-based photocatalysts: A comprehensive review. *Nanoscale* **2021**, *13*, 9463–9504. [CrossRef] [PubMed]
25. Kuang, P.; Low, J.; Cheng, B.; Yu, J.; Fan, J. MXene-based photocatalysts. *J. Mater. Sci. Technol.* **2020**, *56*, 18–44. [CrossRef]
26. Im, J.K.; Sohn, E.J.; Kim, S.; Jang, M.; Son, A.; Zoh, K.-D.; Yoon, Y. Review of MXene-based nanocomposites for photocatalysis. *Chemosphere* **2021**, *270*, 129478. [CrossRef] [PubMed]
27. Khatami, M.; Iravani, P.; Jamalipour Soufi, G.; Iravani, S. MXenes for antimicrobial and antiviral applications: Recent advances. *Mater. Technol. Adv. Perform. Mater.* **2022**, *37*, 1890–1905. [CrossRef]
28. Khatami, M.; Iravani, S. MXenes and MXene-based Materials for the Removal of Water Pollutants: Challenges and Opportunities. *Comments Inorg. Chem.* **2021**, *41*, 213–248. [CrossRef]
29. Zhang, S.; Bilal, M.; Adeel, M.; Barceló, D.; Iqbal, H.M.N. MXene-based designer nanomaterials and their exploitation to mitigate hazardous pollutants from environmental matrices. *Chemosphere* **2021**, *283*, 131293. [CrossRef] [PubMed]
30. Bai, X.; Hou, S.; Wang, X.; Hao, D.; Sun, B.; Jia, T.; Shi, R.; Ni, B.-J. Mechanism of surface and interface engineering under diverse dimensional combinations: The construction of efficient nanostructured MXene-based photocatalysts. *Catal. Sci. Technol.* **2021**, *11*, 5028–5049. [CrossRef]
31. Wojciechowski, T.; Rozmysłowska-Wojciechowska, A.; Matyszczak, G.; Wrzecionek, M.; Olszyna, A.; Peter, A.; Mihaly-Cozmuta, A.; Nicula, C.; Mihaly-Cozmuta, L.; Podsiadło, S.; et al. Ti2C MXene Modified with Ceramic Oxide and Noble Metal Nanoparticles: Synthesis, Morphostructural Properties, and High Photocatalytic Activity. *Inorg. Chem.* **2019**, *58*, 7602–7614. [CrossRef] [PubMed]
32. Makola, L.C.; Moeno, S.; Ouma, C.N.M.; Sharma, A.; Vo, D.-V.N.; Dlamini, L.N. Facile fabrication of a metal-free 2D–2D Nb2CTx@g-C3N4 MXene-based Schottky-heterojunction with the potential application in photocatalytic processes. *J. Alloy. Compd.* **2022**, *916*, 165459. [CrossRef]
33. Sun, Y.; Zhou, Y.; Liu, Y.; Wu, Q.; Zhu, M.; Huang, H.; Liu, Y.; Shao, M.; Kang, Z. A photoactive process cascaded electrocatalysis for enhanced methanol oxidation over Pt-MXene-TiO2 composite. *Nano Res.* **2020**, *13*, 2683–2690. [CrossRef]
34. Hasija, V.; Raizada, P.; Sudhaik, A.; Sharma, K.; Kumar, A.; Singh, P.; Jonnalagadda, S.B.; Thakur, V.K. Recent advances in noble metal free doped graphitic carbon nitride based nanohybrids for photocatalysis of organic contaminants in water: A review. *Appl. Mater. Today* **2019**, *15*, 494–524. [CrossRef]
35. Soni, V.; Singh, P.; Phan Quang, H.H.; Parwaz Khan, A.A.; Bajpai, A.; Van Le, Q.; Thakur, V.K.; Thakur, S.; Nguyen, V.-H.; Raizada, P. Emerging architecture titanium carbide (Ti3C2Tx) MXene based photocatalyst toward degradation of hazardous pollutants: Recent progress and perspectives. *Chemosphere* **2022**, *293*, 133541. [CrossRef]
36. Hoai Ta, Q.T.; Tran, N.M.; Noh, J.-S. Rice crust-like ZnO/Ti3C2Tx MXene hybrid structures for improved photocatalytic activity. *Catalysts* **2020**, *10*, 1140.
37. Ihsanullah, I. MXenes as next-generation materials for the photocatalytic degradation of pharmaceuticals in water. *J. Environ. Chem. Eng.* **2022**, *10*, 107381. [CrossRef]
38. Tu, W.; Liu, Y.; Chen, M.; Zhou, Y.; Xie, Z.; Ma, L.; Li, L.; Yang, B. Carbon nitride coupled with Ti3C2-Mxene derived amorphous Ti-peroxo heterojunction for photocatalytic degradation of rhodamine B and tetracycline. *Colloids Surf. A Physicochem. Eng. Asp.* **2022**, *640*, 128448. [CrossRef]
39. Liu, T.; Li, L.; Geng, X.; Yang, C.; Zhang, X.; Lin, X.; Lv, P.; Mu, Y.; Huang, S. Heterostructured MXene-derived oxides as superior photocatalysts for MB degradation. *J. Alloys Compd.* **2022**, *919*, 165629. [CrossRef]
40. Cui, C.; Guo, R.; Ren, E.; Xiao, H.; Lai, X.; Qin, Q.; Jiang, S.; Shen, H.; Zhou, M.; Qin, W. Facile hydrothermal synthesis of rod-like Nb2O5/Nb2CTx composites for visible-light driven photocatalytic degradation of organic pollutants. *Environ. Res.* **2021**, *193*, 110587. [CrossRef]
41. Shahzad, A.; Rasool, K.; Nawaz, M.; Miran, W.; Jang, J.; Moztahida, M.; Mahmoud, K.A.; Lee, D.S. Heterostructural TiO2/Ti3C2Tx (MXene) for photocatalytic degradation of antiepileptic drug carbamazepine. *Chem. Eng. J.* **2018**, *349*, 748–755. [CrossRef]
42. Iqbal, M.A.; Ali, S.I.; Amin, F.; Tariq, A.; Iqbal, M.Z.; Rizwan, S. La- and Mn-Codoped Bismuth Ferrite/Ti3C2 MXene Composites for Efficient Photocatalytic Degradation of Congo Red Dye. *ACS Omega* **2019**, *4*, 8661–8668. [CrossRef]
43. Zhong, Q.; Liu, J.; Wang, Z.; Ghasemi, J.B.; Zhang, G. Ti3C2 MXene/Ag2ZnGeO4 Schottky heterojunctions with enhanced photocatalytic performances: Efficient charge separation and mechanism studies. *Sep. Purif. Technol.* **2021**, *278*, 119560. [CrossRef]
44. Chen, W.; Wu, B.; Yao, Q.; Dong, G.; Zuo, C.; Zhang, Y.; Zhou, Y.; Liu, Y.; Zhang, Z. A MXene-based multiple catalyst for highly efficient photocatalytic removal of nitrate. *Environ. Sci. Pollut. Res.* **2022**, *29*, 58149–58160. [CrossRef] [PubMed]
45. Jang, J.; Shahzad, A.; Woo, S.H.; Lee, D.S. Magnetic Ti3C2Tx (Mxene) for diclofenac degradation via the ultraviolet/chlorine advanced oxidation process. *Environ. Res.* **2020**, *182*, 108990. [CrossRef] [PubMed]
46. Liu, N.; Lu, N.; Yu, H.; Chen, S.; Quan, X. Efficient day-night photocatalysis performance of 2D/2D Ti3C2/Porous g-C3N4 nanolayers composite and its application in the degradation of organic pollutants. *Chemosphere* **2020**, *246*, 125760. [CrossRef]

47. Cao, Y.; Fang, Y.; Lei, X.; Tan, B.; Hu, X.; Liu, B.; Chen, Q. Fabrication of novel CuFe2O4/MXene hierarchical heterostructures for enhanced photocatalytic degradation of sulfonamides under visible light. *J. Hazard. Mater.* **2020**, *387*, 122021. [CrossRef]
48. Wu, S.; Su, Y.; Zhu, Y.; Zhang, Y.; Zhu, M. In-situ growing Bi/BiOCl microspheres on Ti3C2 nanosheets for upgrading visible-light-driven photocatalytic activity. *Appl. Surf. Sci.* **2020**, *520*, 146339. [CrossRef]
49. Wang, W.Y.; Hood, Z.D.; Zhang, X.Y.; Ivanov, I.N.; Bao, Z.H.; Su, T.M.; Jin, M.Z.; Bai, L.; Wang, X.W.; Zhang, R.B.; et al. Construction of 2D BiVO4-CdS-Ti3C2Tx heterostructures for enhanced photo-redox activities. *ChemCatChem* **2020**, *12*, 3496–3503. [CrossRef]
50. Zhong, Q.; Li, Y.; Zhang, G. Two-dimensional MXene-based and MXene-derived photocatalysts: Recent developments and perspectives. *Chem. Eng. J.* **2021**, *409*, 128099. [CrossRef]
51. Chen, Y.; Xie, X.Q.; Xin, X.; Tang, Z.R.; Xu, Y.J. Ti3C2Tx-based three-dimensional hydrogel by a graphene oxide-assisted self-convergence process for enhanced photoredox catalysis. *ACS Nano* **2019**, *13*, 295–304. [CrossRef] [PubMed]
52. Li, J.Y.; Li, Y.H.; Zhang, F.; Tang, Z.R.; Xu, Y.J. Visible-light-driven integrated organic synthesis and hydrogen evolution over 1D/2D CdS-Ti3C2Tx MXene composites. *Appl. Catal. B Environ.* **2020**, *269*, 118783. [CrossRef]
53. Chen, W.; Han, B.; Xie, Y.; Liang, S.; Deng, H.; Lin, Z. Ultrathin Co-Co LDHs nanosheets assembled vertically on MXene: 3D nanoarrays for boosted visible-light-driven CO2 reduction. *Chem. Eng. J.* **2020**, *391*, 123519. [CrossRef]
54. Cao, S.W.; Shen, B.J.; Tong, T.; Fu, J.W.; Yu, J.G. 2D/2D Heterojunction of ultrathin MXene/Bi2WO6 nanosheets for improved photocatalytic CO2 reduction. *Adv. Funct. Mater.* **2018**, *28*, 1800136. [CrossRef]
55. Anasori, B.; Lukatskaya, M.R.; Gogotsi, Y. 2D metal carbides and nitrides (MXenes) for energy storage. *Nat. Rev. Mater.* **2017**, *2*, 16098. [CrossRef]
56. Nan, J.; Guo, X.; Xiao, J.; Li, X.; Chen, W.; Wu, W.; Liu, H.; Wang, Y.; Wu, M.; Wang, G. Nanoengineering of 2D MXene-based materials for energy storage applications. *Small* **2021**, *17*, 1902085. [CrossRef] [PubMed]
57. Li, M.; Lu, J.; Luo, K.; Li, Y.; Chang, K.; Chen, K.; Zhou, J.; Rosen, J.; Hultman, L.; Eklund, P.; et al. Element Replacement Approach by Reaction with Lewis Acidic Molten Salts to Synthesize Nanolaminated MAX Phases and MXenes. *J. Am. Chem. Soc* **2019**, *141*, 4730–4737. [CrossRef]
58. Salim, O.; Mahmoud, K.A.; Pant, K.K.; Joshi, R.K. Introduction to MXenes: Synthesis and characteristics. *Mater. Today Chem.* **2019**, *14*, 100191. [CrossRef]
59. Xu, C.; Wang, L.; Liu, Z.; Chen, L.; Guo, J.; Kang, N.; Ma, X.-L.; Cheng, H.-M.; Ren, W. Large-area high-quality 2D ultrathin Mo2C superconducting crystals. *Nat. Mater.* **2015**, *14*, 1135–1141. [CrossRef]
60. Geng, D.; Zhao, X.; Chen, Z.; Sun, W.; Fu, W.; Chen, J.; Liu, W.; Zhou, W.; Loh, K.P. Direct synthesis of large-area 2D Mo2C on in situ grown graphene. *Adv. Mater.* **2017**, *29*, 1700072. [CrossRef]
61. Sharma, S.K.; Kumar, A.; Sharma, G.; Vo, D.-V.N.; García-Peñas, A.; Moradi, O.; Sillanpää, M. MXenes based nano-heterojunctions and composites for advanced photocatalytic environmental detoxification and energy conversion: A review. *Chemosphere* **2022**, *291*, 132923. [CrossRef] [PubMed]
62. Velempini, T.; Prabakaran, E.; Pillay, K. Recent developments in the use of metal oxides for photocatalytic degradation of pharmaceutical pollutants in water—A review. *Mater. Today Chem.* **2021**, *19*, 100380. [CrossRef]
63. Siwal, S.S.; Sheoran, K.; Mishra, K.; Kaur, H.; Saini, A.K.; Saini, V.; Vo, D.-V.N.; Nezhad, H.Y.; Thakur, V.K. Novel synthesis methods and applications of MXene-based nanomaterials (MBNs) for hazardous pollutants degradation: Future perspectives. *Chemosphere* **2022**, *293*, 133542. [CrossRef] [PubMed]
64. Assad, H.; Fatma, I.; Kumar, A.; Kaya, S.; Vo, D.-V.N.; Al-Gheethi, A.; Sharma, A. An overview of MXene-Based nanomaterials and their potential applications towards hazardous pollutant adsorption. *Chemosphere* **2022**, *298*, 134221. [CrossRef] [PubMed]
65. Biswal, L.; Mohanty, R.; Nayak, S.; Parida, K. Review on MXene/TiO2 nanohybrids for photocatalytic hydrogen production and pollutant degradations. *J. Environ. Chem. Eng.* **2022**, *10*, 107211. [CrossRef]
66. Wang, Q.; Mei, Y.; Zhou, R.; Komarneni, S.; Ma, J. Persulfate activation of CuS@Ti3C2-based MXene with Bi-active centers toward Orange II removal under visible light. *Colloids Surf. A Physicochem. Eng. Asp.* **2022**, *648*, 129315. [CrossRef]
67. Zhang, H.; Li, M.; Zhu, C.; Tang, Q.; Kang, P.; Cao, J. Preparation of magnetic α-Fe2O3/ZnFe2O4@Ti3C2 MXene with excellent photocatalytic performance. *Ceram. Int.* **2020**, *46*, 81–88. [CrossRef]
68. Yao, Z.; Sun, H.; Sui, H.; Liu, X. 2D/2D Heterojunction of R-scheme Ti3C2 MXene/MoS2 Nanosheets for Enhanced Photocatalytic Performance. *Nanoscale Res. Lett.* **2020**, *15*, 78. [CrossRef] [PubMed]
69. Zhang, Y.-Z.; El-Demellawi, J.K.; Jiang, Q.; Ge, G.; Liang, H.; Lee, K.; Dong, X.; Alshareef, H.N. MXene hydrogels: Fundamentals and applications. *Chem. Soc. Rev.* **2020**, *49*, 7229–7251. [CrossRef]
70. Yang, Y.; Cao, Z.; He, P.; Shi, L.; Ding, G.; Wang, R.; Sun, J. Ti3C2Tx MXene-graphene composite films for wearable strain sensors featured with high sensitivity and large range of linear response. *Nano Energy* **2019**, *66*, 104134. [CrossRef]
71. Mostafavi, E.; Iravani, S. MXene-Graphene Composites: A Perspective on Biomedical Potentials. *Nano Micro Lett.* **2022**, *14*, 130. [CrossRef]
72. Han, R.; Wu, P. High-performance graphene oxide nanofiltration membrane with continuous nanochannels prepared by the in situ oxidation of MXene. *J. Mater. Chem* **2019**, *7*, 6475–6481. [CrossRef]
73. Wu, Z.; Liang, Y.; Yuan, X.; Zou, D.; Fang, J.; Jiang, L.; Zhang, J.; Yang, H.; Xiao, Z. MXene Ti3C2 derived Z–scheme photocatalyst of graphene layers anchored TiO2/g–C3N4 for visible light photocatalytic degradation of refractory organic pollutants. *Chem. Eng. J.* **2020**, *394*, 124921. [CrossRef]

74. Xu, J.; Zeng, G.; Lin, Q.; Gu, Y.; Wang, X.; Feng, Z.; Sengupta, A. Application of 3D magnetic nanocomposites: MXene-supported Fe3O4@CS nanospheres for highly efficient adsorption and separation of dyes. *Sci. Total Environ.* **2022**, *822*, 153544. [CrossRef] [PubMed]
75. Lin, P.; Shen, J.; Yu, X.; Liu, Q.; Li, D.; Tang, H. Construction of Ti3C2 MXene/O-doped g-C3N4 2D-2D Schottky-junction for enhanced photocatalytic hydrogen evolution. *Ceram. Int.* **2019**, *45*, 24656–24663. [CrossRef]
76. Lv, Y.; Wang, K.; Li, D.; Li, P.; Chen, X.; Han, W. Rare Ag nanoparticles loading induced surface-enhanced pollutant adsorption and photocatalytic degradation on Ti3C2Tx MXene-based nanosheets. *Chem. Phys.* **2022**, *560*, 111591. [CrossRef]
77. Thirumal, V.; Yuvakkumar, R.; Kumar, P.S.; Ravi, G.; Keerthana, S.P.; Velauthapillai, D. Facile single-step synthesis of MXene@CNTs hybrid nanocomposite by CVD method to remove hazardous pollutants. *Chemosphere* **2022**, *286*, 131733. [CrossRef] [PubMed]
78. Zhang, L.; Ma, P.; Dai, L.; Bu, Z.; Li, X.; Yu, W.; Cao, Y.; Guan, J. Removal of pollutants via synergy of adsorption and photocatalysis over MXene-based nanocomposites. *Chem. Eng. J. Adv.* **2022**, *10*, 100285. [CrossRef]
79. Zhou, W.; Yu, B.; Zhu, J.; Li, K.; Tian, S. Hierarchical ZnO/MXene (Nb2C and V2C) heterostructure with efficient electron transfer for enhanced photocatalytic activity. *Appl. Surf. Sci.* **2022**, *590*, 153095. [CrossRef]
80. Sun, B.; Tao, F.; Huang, Z.; Yan, W.; Zhang, Y.; Dong, X.; Wu, Y.; Zhou, G. Ti3C2 MXene-bridged Ag/Ag3PO4 hybrids toward enhanced visible-light-driven photocatalytic activity. *Appl. Surf. Sci.* **2021**, *535*, 147354. [CrossRef]
81. Zou, X.; Zhao, X.; Zhang, J.; Lv, W.; Qiu, L.; Zhang, Z. Photocatalytic degradation of ranitidine and reduction of nitrosamine dimethylamine formation potential over MXene–Ti3C2/MoS2 under visible light irradiation. *J. Hazard. Mater.* **2021**, *413*, 125424. [CrossRef]
82. Kumar, A.; Majithia, P.; Choudhary, P.; Mabbett, I.; Kuehnel, M.; Pitchaimuthu, S.; Krishnan, V. MXene coupled graphitic carbon nitride nanosheets based plasmonic photocatalysts for removal of pharmaceutical pollutant. *Chemosphere* **2022**, 136297. [CrossRef] [PubMed]
83. Lai, Y.-J.; Lee, D.-J. Pollutant degradation with mediator Z-scheme heterojunction photocatalyst in water: A review. *Chemosphere* **2021**, *282*, 131059. [CrossRef] [PubMed]
84. Stelo, F.; Kublik, N.; Ullah, S.; Wender, H. Recent advances in Bi2MoO6 based Z-scheme heterojunctions for photocatalytic degradation of pollutants. *J. Alloys Compd.* **2020**, *829*, 154591. [CrossRef]
85. Zhang, G.; Wang, Z.; Wu, J. Construction of a Z-scheme heterojunction for high-efficiency visible-light-driven photocatalytic CO2 reduction. *Nanoscale* **2021**, *13*, 4359–4389. [CrossRef] [PubMed]
86. Zhou, Y.; Yu, M.; Zhan, R.; Wang, X.; Peng, G.; Niu, J. Ti3C2 MXene-induced interface electron separation in g-C3N4/Ti3C2 MXene/MoSe2 Z-scheme heterojunction for enhancing visible light-irradiated enoxacin degradation. *Sep. Purif. Technol.* **2021**, *275*, 119194. [CrossRef]
87. Cao, Z.; Su, J.; Li, Y.; Li, J.; Wang, Z.; Li, M.; Fan, B.; Shao, G.; Wang, H.; Xu, H.; et al. High-energy ball milling assisted one-step preparation of g-C3N4/TiO2@Ti3C2 composites for effective visible light degradation of pollutants. *J. Alloys Compd.* **2021**, *889*, 161771. [CrossRef]
88. Cai, T.; Wang, L.; Liu, Y.; Zhang, S.; Dong, W.; Chen, H.; Yi, X.; Yuan, J.; Xia, X.; Liu, C.; et al. Ag3PO4/Ti3C2 MXene interface materials as a Schottky catalyst with enhanced photocatalytic activities and anti-photocorrosion performance. *Appl. Catal. B Environ.* **2018**, *239*, 545–554. [CrossRef]
89. Long, R.; Yu, Z.; Tan, Q.; Feng, X.; Zhu, X.; Li, X.; Wang, P. Ti3C2 MXene/NH2-MIL-88B(Fe): Research on the adsorption kinetics and photocatalytic performance of an efficient integrated photocatalytic adsorbent. *Appl. Surf. Sci.* **2021**, *570*, 151244. [CrossRef]
90. Vigneshwaran, S.; Park, C.M.; Meenakshi, S. Designed fabrication of sulfide-rich bi-metallic-assembled MXene layered sheets with dramatically enhanced photocatalytic performance for Rhodamine B removal. *Sep. Purif. Technol.* **2021**, *258*, 118003. [CrossRef]